Entropy and Energy Detection-based Spectrum Sensing over F Composite Fading Channels

Published in:
IEEE Transactions on Communications

Document Version:
Peer reviewed version

Queen's University Belfast - Research Portal:
Link to publication record in Queen's University Belfast Research Portal

Entropy and Energy Detection-based Spectrum Sensing over $\mathcal{F}$ Composite Fading Channels

Seong Ki Yoo, *Member, IEEE,* Paschalis C. Sofotasios, *Senior Member, IEEE,*
Simon L. Cotton, *Senior Member, IEEE,* Sami Muhaidat, *Senior Member, IEEE,*
Osamah S. Badarneh, *Member, IEEE,* and George K. Karagiannidis, *Fellow, IEEE*

Abstract—In this paper, we investigate the performance of energy detection-based spectrum sensing over $\mathcal{F}$ composite fading channels. To this end, an analytical expression for the average detection probability is firstly derived. This expression is then extended to account for collaborative spectrum sensing, square-law selection diversity reception and noise power uncertainty. The corresponding receiver operating characteristics (ROC) are analyzed for different conditions of the average signal-to-noise ratio (SNR), noise power uncertainty, time-bandwidth product, multipath fading, shadowing, number of diversity branches and number of collaborating users. It is shown that the energy detection performance is sensitive to the severity of the multipath fading and amount of shadowing, whereby even small variations in either of these physical phenomena can significantly impact the detection probability. As a figure of merit to evaluate the detection performance, the area under the ROC curve (AUC) is derived and evaluated for different multipath fading and shadowing conditions. Closed-form expressions for the differential entropy and cross entropy are also formulated and assessed for different average SNR, multipath fading and shadowing conditions. Then the relationship between the differential entropy of $\mathcal{F}$ composite fading channels and the corresponding ROC/AUC is examined where it is found that the average number of bits required for encoding a signal becomes small (i.e., low differential entropy) when the detection probability is high or when the AUC is large. The difference between composite fading and traditional small-scale fading is emphasized by comparing the cross entropy for Rayleigh and Nakagami-m fading. A validation of the analytical results is provided through a careful comparison with the results of some simulations.

Index Terms—Area under curve, diversity reception, energy detection, entropy, $\mathcal{F}$ composite fading channel, noise power uncertainty, receiver operating characteristics.

I. INTRODUCTION

THE detection of unknown signals is an important issue in many areas of wireless communications such as carrier-sense multiple access based networks, radio detection and ranging (RADAR) systems and cognitive radio [1]. Also, it is expected to be useful in numerous emerging wireless technologies, such as in vehicle-to-vehicle communications, as well as in Internet-of-Things (IoT) based applications, where numerous devices are expected to perform sensing in order to communicate to each-other or with other systems or networks [2–4]. As a result, there have been a number of signal detection techniques proposed in the literature, e.g., matched filter detection (MFD), cyclostationary feature detection (CFD) and energy detection (ED) [5–8]. Compared to the MFD and CFD techniques, ED is quite attractive as it does not require a priori knowledge of the primary signal, i.e., it is a non-coherent detection method. Thus, ED simply measures the received signal energy level over an observation interval and compares it with a pre-determined threshold to determine the presence or absence of the primary signal. Due to its ease of implementation, ED has understandably gained much attention and has been widely used [8–10]. In particular for cognitive radio, ED is commonly used as a spectrum sensing mechanism in order for the secondary users (SUs) to determine whether a primary user (PU) is present or absent in a given frequency band.

Since the effectiveness of ED-based spectrum sensing is greatly impacted by the fading conditions experienced within the operating environment, its performance has been investigated for a number of commonly encountered fading channels [11–16]. For example, the behavior of ED-based spectrum sensing over traditional fading channels, such as Rayleigh [11], [12], Rician [11], [12] and Nakagami-m [11–15], has been studied in terms of the false alarm probability (P_f) and detection probability (P_d) or equivalently missed-detection probability ($P_m = 1 - P_d$). While all of the aforementioned studies have provided important contributions to the understanding of the performance of ED-based spectrum sensing over fading channels, they are restricted to multipath fading channels only. However, in practice, the wireless signal may not only undergo multipath fading but also simultaneous shadowing.

To take into account concurrent multipath fading and shadowing, several composite fading models have been proposed for conventional and emerging communications channels. Accordingly, the performance of ED-based spectrum sensing has also been evaluated over these composite fading channels [17–

22]. For example, in [17–19], the detection performance was investigated within the context of lognormal-based composite fading channels. However, due to the intractability of the lognormal distribution, the Rayleigh / lognormal [18] and Nakagami-m / lognormal [19] composite fading models were approximated using the semi-analytic mixture gamma (MG) distribution. Moreover, a comprehensive performance analysis of ED-based spectrum sensing over generalized K (K_G) composite fading channels [20] and gamma-shadowed Rician fading channels [21] has been conducted for both single-branch and diversity reception cases. More recently, the performance of ED-based spectrum sensing over κ-μ, η-μ and α-μ fading channels and their respective generalized composite fading channels, namely κ-μ / gamma, η-μ / gamma and α-μ / gamma, has been studied in [16] and [22], respectively. In the latter, again due to the inherent mathematical complexity of the formulations, an MG distribution was employed to approximate semi-analytically these three composite fading models.

More recently, in [23], the authors have proposed the use of the Fisher-Snedecor $\mathcal{F}$ distribution to model composite fading channels in which the root mean square (rms) power of a Nakagami-m signal is assumed to be subject to variations induced by an inverse Nakagami-m random variable (RV). In [23], it was demonstrated that in most cases the $\mathcal{F}$ composite fading model provides a better fit to real-world composite fading channels compared to the K_G composite fading model. Most importantly, when comparing the analytical forms of the key statistical metrics and performance measures, the $\mathcal{F}$ composite fading model shows significantly less complexity than the K_G composite fading model. Motivated by these observations, in this paper, we analyze the performance of ED-based spectrum sensing over $\mathcal{F}$ composite fading channels.[1]

Based on the fact that the entropy of the received signal depends on whether the primary signal is present or absent [25], we also evaluate the differential entropy and cross entropy over $\mathcal{F}$ composite fading channels. In particular, differential entropy constitutes a core part of information theory as varying the involved parameters, i.e., multipath fading, shadowing and average signal-to-noise ratio (SNR), is useful for studying the corresponding impact on the information content. To help with the understanding of the relationship between energy detection and differential entropy, in this paper, the evaluation of differential entropy is carried out in parallel with the quantification of these effects on the detectability of unknown signals in cognitive radio and RADAR systems. This relationship provides important insights on how the energy detection of these signals and their respective information content are simultaneously affected by the incurred composite fading conditions. In addition, the differential entropy is considered a

useful criterion when comparing the ROC and AUC measures as interesting insights can be developed on their behavior and sensitivity on how the differential entropy varies for specific values of ROC and AUC. The main contributions of this paper are summarized as follows:

1) We derive a computationally tractable analytic expression for the average detection probability ($\bar{P}_d$) for ED-based spectrum sensing over $\mathcal{F}$ composite fading channels.
2) We then extend this to the cases of collaborative spectrum sensing and square-law selection (SLS) diversity to improve the detection performance.
3) We analyze the performance of ED-based spectrum sensing over $\mathcal{F}$ composite fading channels using the receiver operating characteristic (ROC) curves. Comprehensive numerical results provide useful insights into the performance of ED over $\mathcal{F}$ composite fading channels for different average SNR levels, time-bandwidth product, multipath fading conditions, shadowing conditions, number of diversity branches and number of collaborative users. Furthermore, we investigate the effect of noise power uncertainty on the detection performance. All of these results will be useful in the design of energy-efficient cognitive radio systems for emerging wireless applications.
4) We derive a closed-form expression for the area under the ROC curve (AUC) and evaluate this for different multipath fading and shadowing conditions.
5) We derive closed-form expressions for the differential entropy and cross entropy over $\mathcal{F}$ composite fading channels.
6) The behavior of the differential entropy and cross entropy is then evaluated for different conditions of the average SNR levels, multipath fading and shadowing conditions. Most importantly, we provide important insights into the relationship between the differential entropy and energy detection performance, i.e., how different fading conditions affect the sensing of the signal energy and its information content. Useful insights are also provided when comparing the ROC and AUC measures as a function of the differential entropy.

The remainder of the paper is organized as follows: In Section II, we briefly review the principle of ED and the statistical characteristics of the $\mathcal{F}$ composite fading model. In Section III, we present analytical expressions for the $\bar{P}_d$ over $\mathcal{F}$ composite fading channels for the cases of single user spectrum sensing, collaborative spectrum sensing, SLS diversity reception and noise power uncertainty. Subsequently, a closed-form expression for the AUC is presented in Section IV. In Section V, we also provide exact closed-form expressions for the differential entropy and cross entropy over $\mathcal{F}$ composite fading channels. Section VI provides some numerical and simulation results while Section VII presents some concluding remarks.

---

[1]During the revision process associated with this manuscript, the authors became aware of an another simultaneous and independent work which has studied ED-based spectrum sensing over $\mathcal{F}$ composite fading channels [24]. It is worth highlighting that in the present manuscript, different to the work performed in [24], we introduce a slight modification to the underlying inverse Nakagami-m PDF used to formulate the PDF of the $\mathcal{F}$ composite fading model. This approach ensures stability across the ensuing performance analysis whereas the expressions proposed in [24] require constrained consideration of the SNR PDF of the $\mathcal{F}$ composite fading model to achieve the same.

II. Energy Detection and the $\mathcal{F}$ Composite Fading Model

A. Energy Detection

The received signal $r(t)$ at the output of an ED circuit can be described as [11]

$$r(t) = \begin{cases} n(t), & H_0 \\ h(t)\,s(t) + n(t), & H_1 \end{cases} \tag{1}$$

where s and n denote the transmitted signal and noise[2] respectively, h represents the complex channel gain and t is the time index. The hypothesis H_0 and H_1 signify the absence of the signal and the presence of the signal, respectively. As shown in Fig. 1, a typical ED set-up consists of a noise pre filter (NPF), squaring device, integrator and threshold unit. The received signal is first filtered by an ideal bandpass filter within a pre-determined bandwidth (W) and then the output of the filter is squared and integrated over an observation interval (T) to produce the test statistic (Y). The corresponding test statistic is compared with a pre-determined threshold (λ).

The test statistic Y can be modeled as a central chi-square RV where the number of degrees of freedom is equal to twice the time-bandwidth product ($u = TW$), i.e., $2u$ degrees of freedom, under hypothesis H_0 [11]. On the other hand, under hypothesis H_1, it is modeled as a non-central chi-square RV with $2u$ degrees of freedom and non-centrality parameter 2γ, where $\gamma = |h|^2 E_s / N_0$ is the SNR with E_s and N_0 denoting the signal energy and single-sided noise power spectral density, respectively. As a result, the corresponding probability density function (PDF) of the test statistic Y can be expressed as [11]:

$$f_Y(y) = \begin{cases} \dfrac{y^{u-1}}{2^u \Gamma(u)} \exp\left(-\dfrac{y}{2}\right), & H_0 \\[2ex] \dfrac{1}{2}\left(\dfrac{y}{2\gamma}\right)^{\frac{u-1}{2}} \exp\left(-\dfrac{2\gamma+y}{2}\right) I_{u-1}\left(\sqrt{2\gamma y}\right), & H_1 \end{cases} \tag{2}$$

where $\Gamma[\cdot]$ denotes the gamma function [26, eq. (8.310.1)] and $I_v(\cdot)$ represents the modified Bessel function of the first kind and order v [27, eq. (9.6.20)]. Based on the test statistic above, the P_f and P_d of ED over AWGN channels are given by [11]

$$P_f = P_r(Y > \lambda | H_0) = \frac{\Gamma(u, \lambda/2)}{\Gamma(u)} \tag{3}$$

and

$$P_d = P_r(Y > \lambda | H_1) = Q_u\left(\sqrt{2\gamma}, \sqrt{\lambda}\right) \tag{4}$$

where $\Gamma(\cdot, \cdot)$ and $Q_u(\cdot, \cdot)$ represent the upper incomplete gamma function [26, eq. (8.350.2)] and the generalized Marcum Q-function [28, eq. (1)], respectively.

B. The $\mathcal{F}$ Composite Fading Model

Similar to the physical signal model proposed for the Nakagami-m fading channel, the received signal in an $\mathcal{F}$ composite fading channel is composed of separable clusters
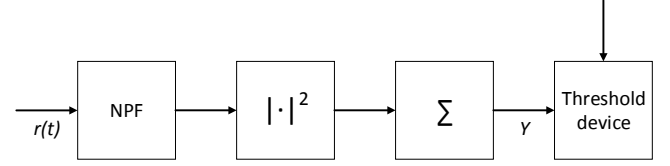
Fig. 1. System model of energy detection [8].

of multipath, in which the scattered waves have similar delay times, with the delay spreads of different clusters being relatively large. However, in contrast to the Nakagami-m signal, in an $\mathcal{F}$ composite fading channel, the rms power of the received signal is subject to random variation induced by shadowing. Following this description, the received signal envelope, R, can be expressed as

$$R^2 = \sum_{n=1}^{m} A^2 I_n^2 + A^2 Q_n^2 \tag{5}$$

where m represents the number of clusters; I_n and Q_n are independent Gaussian RVs with $\mathbb{E}[I_n] = \mathbb{E}[Q_n] = 0$ and $\mathbb{E}[I_n^2] = \mathbb{E}[Q_n^2] = \sigma^2$, with $\mathbb{E}[\cdot]$ denoting the statistical expectation. It is remarking that I_n and Q_n denote the in-phase and quadrature phase components of the cluster n, respectively. In (5), A is a normalized inverse Nakagami-m RV where m_s is the shape parameter and $\mathbb{E}[A^2] = 1$, such that

$$f_A(\alpha) = \frac{2(m_s - 1)^{m_s}}{\Gamma(m_s)\,\alpha^{2m_s + 1}} \exp\left(-\frac{m_s - 1}{\alpha^2}\right). \tag{6}$$

Using the same approach in [23], we can obtain the corresponding PDF of the received signal envelope, R, in an $\mathcal{F}$ fading channel as follows

$$f_R(r) = \frac{2\,m^m (m_s - 1)^{m_s}\,\Omega^{m_s} r^{2m-1}}{B(m, m_s)\,[mr^2 + (m_s - 1)\,\Omega]^{m + m_s}}, \, m_s > 1 \tag{7}$$

where $B(\cdot, \cdot)$ denotes the beta function [26, eq. (8.384.1)]. It is worth highlighting that in this paper, we have slightly modified the underlying inverse Nakagami-m PDF from that used in [23] and subsequently the PDF for the $\mathcal{F}$ composite fading model.[3] The form of the PDF in (7) is functionally equivalent to the $\mathcal{F}$ distribution.[4] In terms of its physical interpretations, m denotes the fading severity whereas m_s controls the amount of shadowing of the rms signal power. Moreover, $\Omega = \mathbb{E}[r^2]$ represents the mean power. As $m_s \to 1$, the scattered signal component undergoes heavy shadowing conditions. In contrast, as $m_s \to \infty$, there exists no shadowing in the channel and therefore it corresponds to a Nakagami-m fading channel. Furthermore, as $m \to \infty$ and $m_s \to \infty$, the $\mathcal{F}$ composite fading model becomes increasingly deterministic, i.e., an AWGN channel.

The corresponding PDF of the instantaneous SNR, γ, in an

$\mathcal{F}$ composite fading channel can be straightforwardly obtained using the transformation of variable $\gamma = \bar{\gamma} r^2/\Omega$, such that

$$f_\gamma(\gamma) = \frac{m^m (m_s-1)^{m_s} \bar{\gamma}^{m_s} \gamma^{m-1}}{B(m, m_s)[m\gamma + (m_s-1)\bar{\gamma}]^{m+m_s}} \qquad (8)$$

where $\bar{\gamma} = \mathbb{E}[\gamma]$ is the average SNR.

III. ENERGY DETECTION OVER $\mathcal{F}$ COMPOSITE FADING CHANNELS

A. Single User Spectrum Sensing

When the signal undergoes fading, the average false alarm probability of ED-based spectrum sensing does not change as P_f is independent of the SNR fading statistics, while the $\bar{P}_d$ of ED can be obtained by averaging over the corresponding SNR fading statistics as follows

$$\bar{P}_d = \int_0^\infty P_d \, f_\gamma(\gamma) \, \mathrm{d}\gamma. \qquad (9)$$

To this end, the $\bar{P}_d$ of ED-based spectrum sensing over $\mathcal{F}$ composite fading channels can be obtained by substituting (4) and (8) into (9), such that

$$\bar{P}_d = \int_0^\infty Q_u\left(\sqrt{2\gamma}, \sqrt{\lambda}\right) \frac{m^m (m_s-1)^{m_s} \bar{\gamma}^{m_s} \gamma^{m-1}}{B(m, m_s)[m\gamma + (m_s-1)\bar{\gamma}]^{m+m_s}} \mathrm{d}\gamma. \qquad (10)$$

Recognizing that the generalized Marcum Q-function in (10) can be equivalently expressed as [29, eq. (29)], namely

$$Q_u\left(\sqrt{2\gamma}, \sqrt{\lambda}\right) = \exp(-\gamma) \sum_{n=0}^\infty \frac{\gamma^n \Gamma(n+u, \lambda/2)}{\Gamma(n+1)\Gamma(n+u)} \qquad (11)$$

then substituting (11) into (10), the $\bar{P}_d$ of ED-based spectrum sensing over $\mathcal{F}$ composite fading channels can be equivalently rewritten as

$$\begin{aligned}\bar{P}_d = \frac{m^m (m_s-1)^{m_s} \bar{\gamma}^{m_s}}{B(m, m_s)} \sum_{n=0}^\infty \frac{\Gamma(n+u, \lambda/2)}{\Gamma(n+1)\Gamma(n+u)} \\ \times \int_0^\infty \frac{\gamma^{n+m-1} \exp(-\gamma)}{[m\gamma + (m_s-1)\bar{\gamma}]^{m+m_s}} \mathrm{d}\gamma. \end{aligned} \qquad (12)$$

With the aid of [26, eq. (3.383.5)] and making use of the generalized Laguerre polynomials [30, eq. (07.03.02.0001.01)][5], the $\bar{P}_d$ can be expressed as (13), at the top of the next page. In (13), $_1F_1(\cdot;\cdot;\cdot)$ represents the Kummer confluent hypergeometric function [26, eq. (9.210.1)]. It is worth noting that [26, eq. (3.383.5)] is only valid when $m + m_s$ is not a positive integer number, i.e., $m + m_s \neq \mathbb{N}$. Nonetheless, this potential singularity can be straightforwardly circumvented by introducing an infinitely small perturbation term that can be added to $m+m_s$, if required. Furthermore, with the aid of [30, eq. (07.20.16.0006.01)], (13) can be rewritten as (14) which is shown at the top of the next page, where $U(\cdot;\cdot;\cdot)$ denotes the confluent hypergeometric function of the second kind.

---

[5]Although the main title of [30] is Wolfram Research, the page title depends on the id specified along with the reference. In the case of [30, eq. (07.03.02.0001.01)], (07.03.02.0001.01) indicates the id. Consequently, http://functions.wolfram.com/07.03.02.0001.01 indicates that the title of the page is LaguerreL (Generalized Laguerre function).

It is noted that the infinite series representation in (14) is convergent and only few terms are required in practice of its truncation. However, in the analysis of digital communications over fading channels, it is essential to determine the exact number of truncation terms to guarantee target performance or quality of service requirements. Based on this, we derive an upper bound for the truncation error of (14), which can be computed straightforwardly because it is expressed in closed-form in terms of known and built-in functions. Based on this, the truncation error, $\mathcal{T}$, for the infinite series in (14) if it is truncated after $T_0 - 1$ terms, is given as

$$\begin{aligned}\mathcal{T} = \sum_{n=T_0}^\infty \frac{\Gamma(n+u, \lambda/2)\Gamma(n+m)}{\Gamma(n+1)\Gamma(n+u)} \\ \times U\left(m+m_s; \, m_s-n+1; \, \frac{(m_s-1)\bar{\gamma}}{m}\right). \end{aligned} \qquad (15)$$

Since the confluent hypergeometric function of the second kind is monotonically decreasing with respect to n, $\mathcal{T}$ can be bounded as

$$\begin{aligned}\mathcal{T} \leq U\left(m+m_s; \, m_s-T_0+1; \, \frac{(m_s-1)\bar{\gamma}}{m}\right) \\ \times \sum_{n=T_0}^\infty \frac{\Gamma(n+u, \lambda/2)\Gamma(n+m)}{\Gamma(n+1)\Gamma(n+u)}. \end{aligned} \qquad (16)$$

With the aid of the monotonicity properties of the upper incomplete gamma function, $\Gamma(a,x) < \Gamma(a,0) = \Gamma(a)$, the above expression can be upper bounded as follows

$$\mathcal{T} < U\left(m+m_s; m_s-T_0+1; \frac{(m_s-1)\bar{\gamma}}{m}\right)\sum_{n=T_0}^\infty \frac{\Gamma(n+m)}{\Gamma(n+1)}. \qquad (17)$$

Since we add up strictly positive terms, the summation above can be rewritten as $\sum_{n=T_0}^\infty \frac{\Gamma(n+m)}{\Gamma(n+1)} \leq \sum_{n=0}^\infty \frac{\Gamma(n+m)}{\Gamma(n+1)}$. To this effect and by also recalling the Pochhammer symbol identities, it follows that

$$\mathcal{T} < U\left(m+m_s; m_s-T_0+1; \frac{(m_s-1)\bar{\gamma}}{m}\right)\sum_{n=0}^\infty \frac{(m)_n \Gamma(m)}{n!}. \qquad (18)$$

It is evident that the above infinite series representations can be expressed in closed-form as

$$\mathcal{T} < U\left(m+m_s; m_s-T_0+1; \frac{(m_s-1)\bar{\gamma}}{m}\right)\Gamma(m)\,_1F_0(m; ; 1) \qquad (19)$$

where $_1F_0(\cdot; \cdot; \cdot)$ is the generalized hypergeometric function.

B. Collaborative Spectrum Sensing

The detection performance of ED-based spectrum sensing can be significantly improved using collaborative spectrum sensing [31], [32] which exploits the spatial diversity among SUs (i.e., sharing their sensing information). For simplicity, we assume that all N collaborative SUs experience independent and identically distributed (i.i.d.) fading and employ the same decision rule (i.e., the same threshold). For the OR-rule or equivalently 1-out-of-n rule, the final decision is made when at least one SU shares a local decision. In this case, the

$$\bar{P}_d = \frac{1}{B(m,m_s)}\sum_{n=0}^{\infty}\frac{\Gamma(n+u,\lambda/2)\Gamma(n-m_s)}{\Gamma(n+1)\,\Gamma(n+u)}\left[\left(\frac{(m_s-1)\,\bar{\gamma}}{m}\right)^{m_s}{}_1F_1\left(m+m_s;m_s-n+1;\frac{(m_s-1)\,\bar{\gamma}}{m}\right)\right.$$
$$\left. + \left(\frac{(m_s-1)\,\bar{\gamma}}{m}\right)^n\frac{B(n+m,m_s-n)}{\Gamma(n-m_s)}{}_1F_1\left(n+m;n-m_s+1;\frac{(m_s-1)\,\bar{\gamma}}{m}\right)\right] \tag{13}$$

$$\bar{P}_d = \frac{(m_s-1)^{m_s}\bar{\gamma}^{m_s}}{B(m,m_s)\,m^{m_s}}\sum_{n=0}^{\infty}\frac{\Gamma(n+u,\lambda/2)\Gamma(n+m)}{\Gamma(n+1)\,\Gamma(n+u)}U\left(m+m_s;m_s-n+1;\frac{(m_s-1)\,\bar{\gamma}}{m}\right) \tag{14}$$

collaborative detection probability (P_d^{OR}) and false alarm probability (P_f^{OR}) under AWGN can be written as follows

$$P_d^{\mathrm{OR}} = 1 - (1-P_d)^N \tag{20}$$

and

$$P_f^{\mathrm{OR}} = 1 - (1-P_f)^N. \tag{21}$$

On the other hand, for the AND-rule, the final decision is made when all SUs share their local decision. In this case, the P_d^{AND} and P_f^{AND} under AWGN can be written as follows

$$P_d^{\mathrm{AND}} = P_d{}^N \tag{22}$$

and

$$P_f^{\mathrm{AND}} = P_f{}^N. \tag{23}$$

Based on this, the average detection probability of ED system over $\mathcal{F}$ composite fading channels with N collaborative SUs can be obtained by substituting (14) into (20) and (22) for the OR- and AND-rule respectively, yielding the following analytical representations given in (24) and (25), which are shown at the top of next page.

C. Square-Law Selection Diversity Reception

Using diversity reception techniques is one of the most well-known methods which can be used to mitigate the deleterious effects of fading in wireless communication systems. Among other competing schemes, SLS diversity reception is efficient and highly regarded due to its simplicity. As shown in Fig. 2, in an SLS scheme, the energy detection process is performed before combining. Consequently, an SLS scheme selects the branch with the highest resultant test statistic, i.e., $Y^{\mathrm{SLS}} = \max\{Y_1,Y_1,\ldots Y_L\}$ [15]. Under hypotheses H_0, the false alarm probability for an SLS scheme (P_f^{SLS}) over AWGN channels can be determined as follows

$$P_f^{\mathrm{SLS}} = 1 - \left[1 - \frac{\Gamma(u,\lambda/2)}{\Gamma(u)}\right]^L \tag{26}$$

where L represents the number of diversity branches. On the contrary, under hypothesis H_1, the detection probability for an L-branch SLS scheme (P_d^{SLS}) over AWGN channels can be expressed as

$$P_d^{\mathrm{SLS}} = 1 - \prod_{i=1}^{L}\left[1 - Q_u\left(\sqrt{2\gamma_i},\sqrt{\lambda}\right)\right]. \tag{27}$$

Consequently, for an L-branch SLS system operating over i.i.d. $\mathcal{F}$ composite fading channels, the average detection
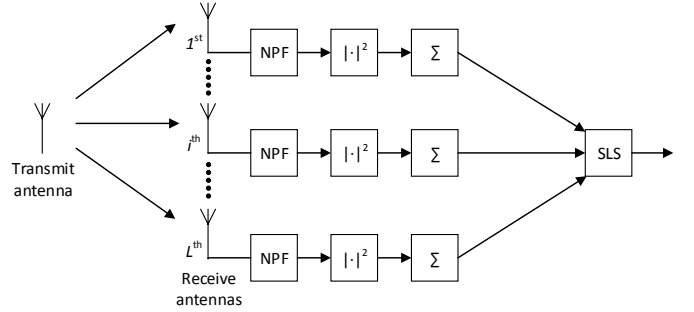

Fig. 2. System model of energy detection for an L-branch SLS diversity scheme [33].

probability, P_d^{SLS}, can be obtained as

$$\bar{P}_d^{\mathrm{SLS}} = 1 - \prod_{i=1}^{L}\int_0^{\infty}\left[1 - Q_u\left(\sqrt{2\gamma_i},\sqrt{\lambda}\right)\right]f_{\gamma_i}(\gamma_i)\,\mathrm{d}\gamma_i$$
$$= 1 - \prod_{i=1}^{L}\left[\int_0^{\infty}f_{\gamma_i}(\gamma_i)\mathrm{d}\gamma_i - \int_0^{\infty}Q_u\left(\sqrt{2\gamma_i},\sqrt{\lambda}\right)f_{\gamma_i}(\gamma_i)\,\mathrm{d}\gamma_i\right]$$
$$= 1 - \prod_{i=1}^{L}\left[1 - \bar{P}_d\left(\gamma_i\right)\right]. \tag{28}$$

By substituting (14) into (28), an analytical expression for P_d^{SLS} is obtained as (29), at the top of the next page

D. Noise Power Uncertainty

In all of the previous cases considered, the detection probability has been grounded on the assumption that the noise power is accurately known. However, in practice, noise power varies with time and location, which is often referred to as the noise power uncertainty [34]. Clearly, any change in the noise power will affect the detection performance, with the main sources of this uncertainty including the non-linearity and the thermal noise of the components in the receiver and environmental noise caused by the transmissions of other wireless users [35–37]. Therefore, in practice, it is very difficult to obtain a precise knowledge of the noise power.

Assuming that the uncertainty in the noise power estimation can be characterized by the term β (which is expressed in decibels), the noise power uncertainty in energy detection can be appropriately modeled as existing in the range $[\sigma_W/\alpha, \alpha\sigma_W]$ where σ_W denotes the nominal noise power

$$\bar{P}_d^{\text{OR}} = 1 - \left[1 - \frac{(m_s-1)^{m_s}\bar{\gamma}^{m_s}}{B(m,m_s)\,m^{m_s}} \sum_{n=0}^{\infty} \frac{\Gamma(n+u,\,\lambda/2)\Gamma(n+m)}{\Gamma(n+1)\,\Gamma(n+u)} U\left(m+m_s; m_s-n+1; \frac{(m_s-1)\,\bar{\gamma}}{m}\right)\right]^N \tag{24}$$

$$\bar{P}_d^{\text{AND}} = \left[\frac{(m_s-1)^{m_s}\bar{\gamma}^{m_s}}{B(m,m_s)m^{m_s}} \sum_{n=0}^{\infty} \frac{\Gamma(n+u,\,\lambda/2)\Gamma(n+m)}{\Gamma(n+1)\,\Gamma(n+u)} U\left(m+m_s; m_s-n+1; \frac{(m_s-1)\,\bar{\gamma}}{m}\right)\right]^N \tag{25}$$

$$\bar{P}_d^{\text{SLS}} = 1 - \prod_{i=1}^{L}\left[1 - \frac{(m_{s_i}-1)^{m_{s_i}}\,\bar{\gamma}_i^{m_{s_i}}}{B(m_i,m_{s_i})\,m_i^{m_{s_i}}} \sum_{n=0}^{\infty} \frac{\Gamma(n+u,\,\lambda/2)\,\Gamma(n+m_i)}{\Gamma(n+1)\,\Gamma(n+u)} U\left(m_i+m_{s_i}; m_{s_i}-n+1; \frac{(m_{s_i}-1)\,\bar{\gamma}_i}{m_i}\right)\right] \tag{29}$$

and $\alpha = 10^{\beta/10} > 1$ quantifies the size of the uncertainty [34]. Therefore, when the noise power is overestimated as $\bar{\sigma}_W = \alpha\sigma_W$ (i.e., for the worst case scenario), the detection probability can be obtained as [38]

$$P_d^{\text{NU}} = Q_u\left(\sqrt{2\gamma},\, \sqrt{\alpha^2\lambda}\right). \tag{30}$$

Hence, to evaluate the performance of (30) over $\mathcal{F}$ composite fading channels, the average detection probability, $\bar{P}_d^{\text{NU}}$, can be directly obtained by scaling the detection threshold with the noise uncertainty, i.e., λ is replaced by $\alpha^2\lambda$ in (14).

IV. Average Area Under the ROC Curve for $\mathcal{F}$ Composite Fading Channels

The ROC curve is usually employed to evaluate the detection performance. However, for multiple energy detectors, it is difficult to visually compare their performance based on their ROC curves. Following the Area Theorem presented in [39], the AUC can be used as an alternative measure of detection capability, where the AUC is simply defined as the area covered by the ROC curve. This represents the probability of choosing the correct decision at the detector is more likely than choosing the incorrect decision [40], [41]. As the threshold used in the detector varies from ∞ to 0, the AUC varies from 0.5 (poor performance) to 1 (good performance).

A. AUC for the Instantaneous SNR

Let $A(\gamma)$ denote the AUC which is a function of instantaneous SNR value γ. For the ROC curve of P_d versus P_f, $A(\gamma)$ can be evaluated as [42]

$$A(\gamma) = \int_0^1 P_d(\gamma, \lambda)\, dP_f(\lambda). \tag{31}$$

As both $P_d(\gamma, \lambda)$ and $P_f(\lambda)$ are functions of the threshold λ, we can use the threshold averaging method [43] to calculate the AUC. When the value of $P_f(\lambda)$ varies from 0 to 1 ($0 \to 1$), it is equivalent to λ ranging from ∞ to 0 ($\infty \to 0$). Consequently, (31) can be rewritten as

$$A(\gamma) = -\int_0^{\infty} P_d(\gamma, \lambda) \frac{\partial P_f(\lambda)}{\partial \lambda}\, d\lambda \tag{32}$$

where $\frac{\partial P_f(\lambda)}{\partial \lambda}$ denotes the partial derivative of P_f with respect to λ, which is obtained from (3)

$$\frac{\partial P_f(\lambda)}{\partial \lambda} = -\frac{\lambda^{u-1}}{2^u\Gamma(u)}\exp\left(-\frac{\lambda}{2}\right). \tag{33}$$

By substituting (4) and (33) into (32), $A(\gamma)$ is expressed as

$$A(\gamma) = \sum_{n=0}^{\infty} \frac{\gamma^n\exp(-\gamma)}{2^u\Gamma(u)\,\Gamma(n+1)\,\Gamma(n+u)} \times \int_0^{\infty}\lambda^{u-1}\exp\left(-\frac{\lambda}{2}\right)\Gamma(n+u,\,\lambda/2)\,d\lambda \tag{34}$$

which with the aid of [44, eq. (12)], it can be obtained as

$$A(\gamma) = 1 - \sum_{l=0}^{u-1}\sum_{i=0}^{l}\binom{l+u-1}{l-i}\frac{\gamma^i}{i!\,2^{l+u+i}}\exp\left(-\frac{\gamma}{2}\right) \tag{35}$$

where $\binom{a}{b}$ represents the binomial coefficient.

B. Average AUC for $\mathcal{F}$ Composite Fading Channels

The corresponding average AUC $(\bar{A})$ for $\mathcal{F}$ composite fading channels can be evaluated through averaging (35) by the corresponding SNR fading statistics, such that [42]

$$\bar{A} = \int_0^{\infty} A(\gamma)\, f_\gamma(\gamma)\, d\gamma. \tag{36}$$

Substituting (8) and (35) into (36), $\bar{A}$ can be expressed as

$$\bar{A} = 1 - \sum_{l=0}^{u-1}\sum_{i=0}^{l}\binom{l+u-1}{l-i}\frac{m^m(m_s-1)^{m_s}\bar{\gamma}^{m_s}}{i!\,2^{l+u+i}B(m,m_s)} \times \int_0^{\infty}\frac{\gamma^{m+i-1}\exp\left(-\frac{\gamma}{2}\right)}{[m\gamma+(m_s-1)\bar{\gamma}]^{m+m_s}}\,d\gamma. \tag{37}$$

Since the integral in (37) is the same form as that given in (12), $\bar{A}$ can be similarly obtained with the aid of [26, eq. (3.383.5)] and [30, eq. (07.20.16.0006.01)], such that

$$\bar{A} = 1 - \sum_{l=0}^{u-1}\sum_{i=0}^{l}\binom{l+u-1}{l-i}\frac{(m_s-1)^{m_s}\bar{\gamma}^{m_s}\Gamma(m+i)}{i!\,2^{l+u+m_s}m^m B(m,m_s)} \times U\left(m+m_s; m_s-i+1; \frac{(m_s-1)\bar{\gamma}}{2m}\right) \tag{38}$$

which is expressed by an exact closed-form expression that involves known functions that are built-in in popular software packages such as Maple, Matlab and Mathematica.

V. Entropy for $\mathcal{F}$ Composite Fading Channels

A. Differential Entropy

It is recalled that the differential entropy denotes the amount of information contained in a signal and indicates the average

number of bits required for encoding this information. For continuous RVs with PDF, $p_X(x)$, it is given by $H(p) = -\int_0^\infty p_X(x) \log_2(p_X(x)) \, dx$ [45]. Thus, for the case of $\mathcal{F}$ composite fading channels, it can be expressed by substituting (8) into $p_X(x)$, such that

$$H(p) = -\int_0^\infty \frac{m^m (m_s-1)^{m_s} \bar{\gamma}^{m_s} \gamma^{m-1}}{B(m, m_s) [m\gamma + (m_s-1)\bar{\gamma}]^{m+m_s}}$$
$$\times \log_2\left(\frac{m^m (m_s-1)^{m_s} \bar{\gamma}^{m_s} \gamma^{m-1}}{B(m, m_s) [m\gamma + (m_s-1)\bar{\gamma}]^{m+m_s}}\right) d\gamma. \quad (39)$$

Using the logarithmic identities and after some algebraic manipulations, (39) can be rewritten as (40) which is shown at the top of the next page, Performing a simple transformation of variables and applying [26, eq. (4.293.14)] along with some algebraic manipulation, (40) can be expressed in closed-form, such that

$$H(p) = \frac{(m+m_s)\psi(m+m_s) - (m-1)\psi(m) - (m_s+1)\psi(m_s)}{\ln(2)}$$
$$+ \log_2\left[\frac{B(m, m_s)(m_s-1)\bar{\gamma}}{m}\right] \quad (41)$$

where $\psi(\cdot)$ represents the psi (polygamma) function [26, eq. (8.360)]. Similar to the average detection probability and AUC, as shown in (41), the differential entropy is also expressed in terms of the m, m_s and $\bar{\gamma}$ parameters. This may suggest that there exist a relationship between the energy and the information content of a signal. It should be noted that a similar expression to (41) was presented in [46], [47]. Nevertheless, (41) provides useful insights as it is based on the physical parameters of the $\mathcal{F}$ composite fading model, i.e., m (multipath fading severity), m_s (shadowing severity) and $\bar{\gamma}$ (average SNR).

B. Cross Entropy

The cross entropy measures the average number of bits required to encode a message when a distribution $p_X(x)$ is replaced by a distribution $q_X(x)$. The cross entropy between two continuous RVs with PDFs $p_X(x)$ and $q_X(x)$ is given by $H(p,q) = -\int_0^\infty p_X(x) \log_2(q_X(x)) \, dx$ [45]. In the present analysis, $p_X(x)$ represents the $\mathcal{F}$ distribution while the Rayleigh and Nakagami-m distributions are considered for $q_X(x)$. To understand what happens when composite fading is not taken into account, the corresponding cross entropy with respect to the Rayleigh and Nakagami-m distributions are respectively given by

$$H_{\text{Ray}}(p,q) = -\int_0^\infty \frac{m^m (m_s-1)^{m_s} \bar{\gamma}^{m_s} \gamma^{m-1}}{B(m, m_s) [m\gamma + (m_s-1)\bar{\gamma}]^{m+m_s}}$$
$$\times \log_2\left(\frac{1}{\bar{\gamma}_R} \exp\left(-\frac{\gamma}{\bar{\gamma}_R}\right)\right) d\gamma \quad (42)$$

and

$$H_{\text{Nak}}(p,q) = -\int_0^\infty \frac{m^m (m_s-1)^{m_s} \bar{\gamma}^{m_s} \gamma^{m-1}}{B(m, m_s) [m\gamma + (m_s-1)\bar{\gamma}]^{m+m_s}}$$
$$\times \log_2\left(\frac{\hat{m}^{\hat{m}} \gamma^{\hat{m}-1}}{\Gamma(\hat{m}) \bar{\gamma}_N^{\hat{m}}} \exp\left(-\frac{\hat{m}\gamma}{\bar{\gamma}_N}\right)\right) d\gamma \quad (43)$$

where $\bar{\gamma}_R$ is the average SNR of the Rayleigh distribution, $\hat{m}$ and $\bar{\gamma}_N$ denote the fading severity parameter and average SNR of the Nakagami-m distribution, respectively. In a similar manner to Section V.A, by performing the necessary transformation of variables and applying [26, eq. (3.194.3)] and [26, eq. (4.293.14)] along with some algebraic manipulation, (42) and (43) can be expressed in closed-form as follows

$$H_{\text{Ray}}(p,q) = \log_2(\bar{\gamma}_R) + \frac{\bar{\gamma}}{\ln(2)\bar{\gamma}_R} \quad (44)$$

and

$$H_{\text{Nak}}(p,q) = \frac{\hat{m}\bar{\gamma}}{\ln(2)\bar{\gamma}_N} - \log_2\left(\frac{\hat{m}^{\hat{m}}}{\Gamma(\hat{m})\bar{\gamma}_N^{\hat{m}}}\right)$$
$$+ \frac{\hat{m}-1}{\ln(2)}\left[\ln\left(\frac{m}{(m_s-1)\bar{\gamma}}\right) - \psi(m) + \psi(m_s)\right]. \quad (45)$$

It is noted that (42) and (46) can be computed straightforwardly since $\psi(\cdot)$ is included as a built-in function in most popular scientific software packages.

VI. Numerical and Simulation Results

Capitalizing on the derived analytic results, we next quantify the effects of $\mathcal{F}$ composite fading conditions for different communication scenarios and fading severity conditions. It is worth remarking that the number of terms utilized in the numerical results was 101.[6]

A. Energy Detection

We firstly analyze the performance of ED-based spectrum sensing over $\mathcal{F}$ composite fading channels in terms of the corresponding ROC curves. As an example, Fig. 3 shows the ROC curves for different values of the average SNR ($\bar{\gamma}$), time-bandwidth product (u), multipath fading (m) and shadowing (m_s) parameters. It can be seen that the performance of ED-based spectrum sensing improves when the average SNR increases (higher values of $\bar{\gamma}$), or when the time-bandwidth product decreases (lower values of u), or when the severity of multipath fading and shadowing decreases (higher values of m and m_s). It is worth remarking that we have also included the results of some simulations (shown as symbols) in Fig. 3, which were performed to validate the derived analytic expressions. Owing to the simplicity of the $\mathcal{F}$ composite fading model, these simulated sequences, each consisting of 100,000 realizations, were straightforwardly generated in MATLAB through the calculation of the ratio of two gamma RVs.

The $\mathcal{F}$ composite fading model inherit all of the generality of the Nakagami-m fading model [11]. Thus, it includes as special cases the Nakagami-m and Rayleigh fading models. More specifically, in the absence of shadowing in the channel (i.e., $m_s \to \infty$), the $\mathcal{F}$ composite fading model coincides with the Nakagami-m fading model. Likewise, the Rayleigh fading model is readily obtained by setting $m = 1$ and $m_s \to \infty$. Consequently, some of the special cases of the ROC curves

---

[6]With 101 truncation terms, the numerical results provided a good accuracy. For instance, when compared to the $\bar{P}_d$ values computed using (10) and (14), the truncation error was found to be approximately 2.31704×10^{-12}.

$$H(p) = -\log_2\left[\frac{m^m(m_s-1)^{m_s}\bar{\gamma}^{m_s}}{B(m,m_s)}\right] - \frac{m^m(m_s-1)^{m_s}\bar{\gamma}^{m_s}}{B(m,m_s)\ln(2)}$$
$$\times\left[\int_0^\infty \frac{\gamma^{m-1}\ln(\gamma^{m-1})}{[m\gamma+(m_s-1)\bar{\gamma}]^{m+m_s}}\mathrm{d}\gamma - \int_0^\infty \frac{\gamma^{m-1}\ln\left([m\gamma+(m_s-1)\bar{\gamma}]^{m+m_s}\right)}{[m\gamma+(m_s-1)\bar{\gamma}]^{m+m_s}}\mathrm{d}\gamma\right] \tag{40}$$
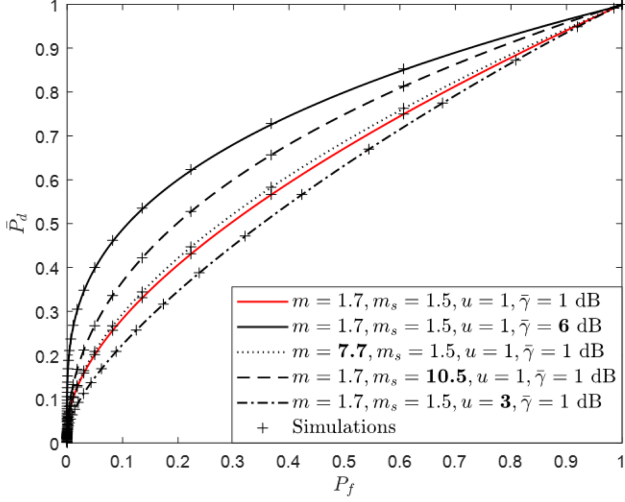

Fig. 3. ROC curves for $\mathcal{F}$ composite fading channels considering different $\bar{\gamma}$, m, m_s and u values.
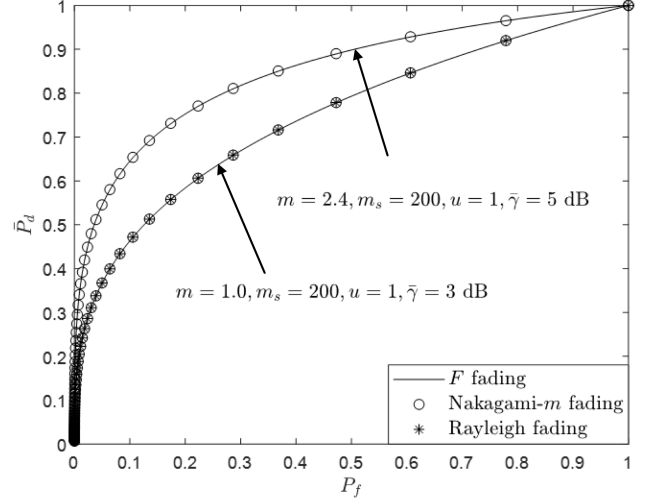

Fig. 4. ROC curves for some special cases of the $\mathcal{F}$ composite fading channel: Rayleigh (asterisks) and Nakagami-m (circles).

which coincide with those for the Rayleigh and Nakagami-m fading channels are illustrated in Fig. 4 as a further validations and insights. It is evident that the considered composite model is more versatile as it can effectively account for the difference between Rayleigh and Nakagami-m fading conditions, leading to more accurate and reliable results. The versatility is further evident by the fact that this model can also account for shadowing, unlike the standard Nakagami-m and Rayleigh fading models.

Fig. 5 illustrates the ROC curves for collaborative ED-based spectrum sensing with $N = 2, 4, 8$ using the OR and AND rules with $m = 3.5$, $m_s = 4.3$, $\bar{\gamma} = 3$ dB and $u = 2$. For comparison, the ROC curve for non-collaborative ED-based spectrum sensing (i.e., single user spectrum sensing) is also shown in Fig. 5. As expected, the energy detection performance improves as the number of collaborative SUs increases. It is also observed that the OR rule provides a better performance compared to the AND rule. Fig. 6 shows the detection performance variation with increasing number of diversity branches (L) and time-bandwidth product (u) for an L-branch SLS scheme. It is clear that lower u and higher L provides a better performance. Furthermore, when $L = 1$ the ROC curves for an L-branch SLS scheme become equivalent to those for $\mathcal{F}$ composite fading channel. Again, the simulation results provide a perfect match to the analytical results presented in Fig. 5 and Fig. 6.

Fig. 7 demonstrates how the detection performance varies with $\bar{\gamma}$ over $\mathcal{F}$ composite fading channels with $m = 1.3$, $m_s = 2.7$, $u = 2$ and $\lambda = 7.78$ under a number of different conditions of noise power uncertainty. It is apparent that the
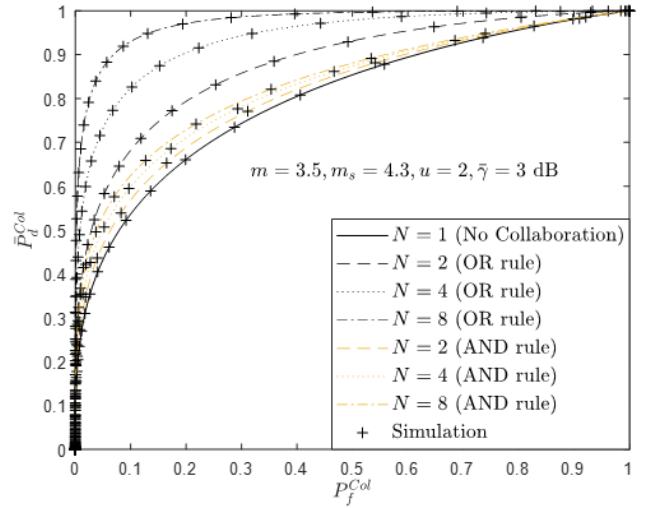

Fig. 5. ROC curves for collaborative ED-based spectrum sensing with OR and AND rules over $\mathcal{F}$ composite fading channels, with $m = 3.5$, $m_s = 4.3$, $\bar{\gamma} = 3$ dB, $u = 2$ and N collaborating users with $N = 2$, 4 and 8.

detection performance decreases as noise uncertainty increases and the effects of noise uncertainty are non negligible. For example, the value of $\bar{P}_d^{\mathrm{NU}}$ for $\bar{\gamma} = 6$ dB and $\beta = 0$ dB (i.e., perfect noise power estimation) was approximately 0.52 while the value of $\bar{P}_d^{\mathrm{NU}}$ for $\beta = 2$ dB was found to be approximately 0.15. Furthermore, to achieve $\bar{P}_d^{\mathrm{NU}} = 0.9$, the ED-based spectrum sensing with $\beta = 2$ dB requires an additional 5 dB compared to when $\beta = 0$ dB. To illustrate both the isolated and combined effects of multipath and shadowing on the AUC for $\mathcal{F}$ composite fading channels, Fig. 8 shows the estimated
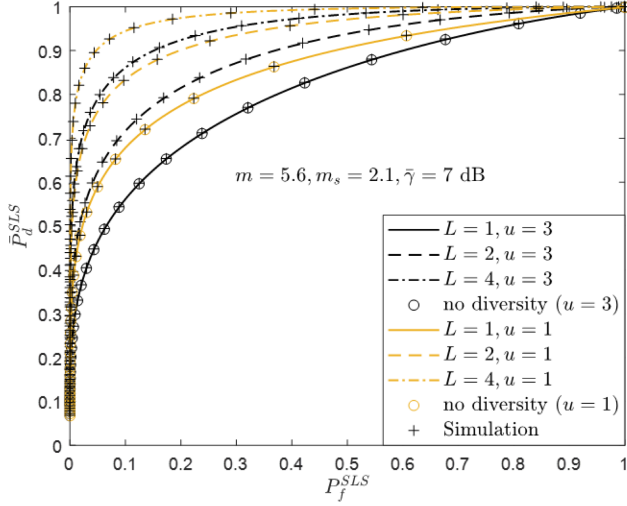
Fig. 6. ROC curves for an L-branch SLS system with $L = 1, 2$ and 4 over i.i.d. $\mathcal{F}$ composite fading channels, with $m = 5.6$, $m_s = 1.1$, $\bar{\gamma} = 7$ dB and $u = \{1, 3\}$.

Fig. 8. Average AUC in an $\mathcal{F}$ composite fading channel as a function of the multipath fading (m) and shadowing (m_s) parameters, with $u = 2$ and $\bar{\gamma} = 2$ dB.
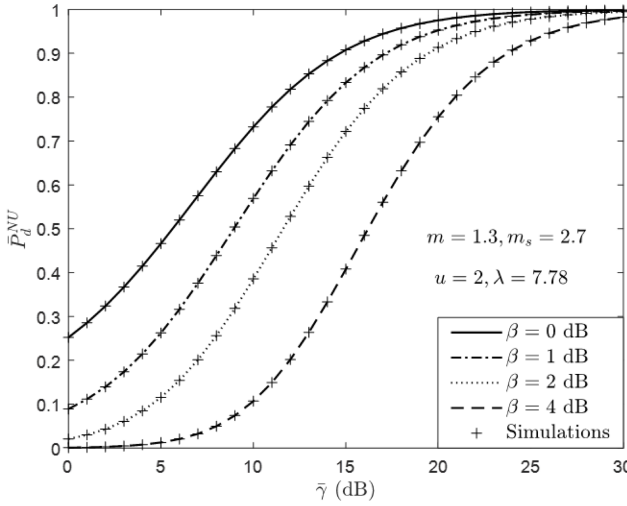

Fig. 7. Average detection probability ($\bar{P}_d^{NU}$) versus average SNR ($\bar{\gamma}$) over $\mathcal{F}$ composite fading channels, with $m = 1.3$, $m_s = 2.7$, $u = 2$ and $\lambda = 7.78$ under different conditions of noise power uncertainty.

Fig. 9. Differential entropy in an $\mathcal{F}$ composite fading channel as a function of its key parameters: multipath fading (m), shadowing (m_s) and average SNR ($\bar{\gamma}$).

AUC values for different multipath fading ($1.0 \leq m \leq 15$) and shadowing ($2.0 \leq m_s \leq 15$) conditions, with $u = 2$ and $\bar{\gamma} = 2$ dB. It is clear that smaller values of the AUC (close to 0.5) occurred when the channel was subject to simultaneous heavy shadowing ($m_s \to 2$) and severe multipath fading ($m \to 1$), i.e., intense composite fading, whereas the higher AUC values (close to 1) appeared when both the multipath and shadowing parameters became large ($m, m_s \to 15$), i.e., light composite fading.

B. Entropy

Fig. 9 shows the estimated differential entropy for different multipath fading and shadowing intensities of $\mathcal{F}$ composite fading channels, i.e., $3 \leq m \leq 10$, $3 \leq m_s \leq 10$ and 0 dB $\leq \bar{\gamma} \leq 20$ dB. It is obvious that higher values of the differential entropy appear at higher $\bar{\gamma}$, lower m and lower m_s. This may indicate that more bits are required to encode the corresponding message when the channel is subject to higher
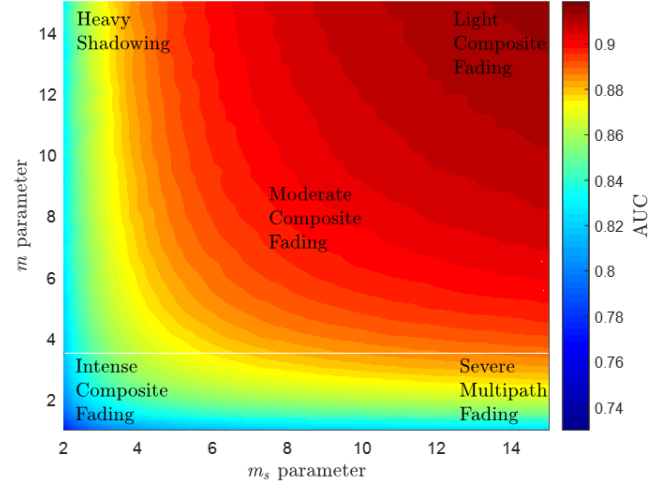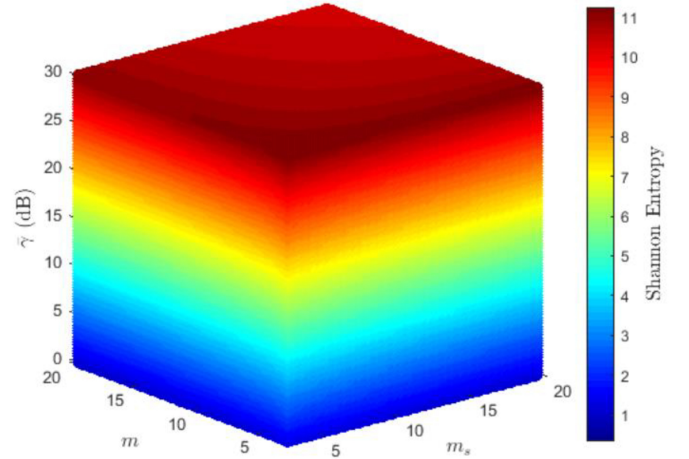
average SNR, severer multipath fading and heavier shadowing. As already shown in Fig. 3 and Fig. 8, the ROC curves and AUC are also highly dependent upon multipath fading and shadowing conditions experienced in $\mathcal{F}$ composite fading channels. Motivated by this, we compare the behavior of the differential entropy and ROC curves.

Fig. 10 shows the estimated differential entropy and ROC curves as a function of (a) average SNR ($\bar{\gamma}$) with fixed fading parameters $m = m_s = \{2, 10\}$ and $u = 2$; (b) multipath fading (m) with $\bar{\gamma} = \{5, 15\}$ dB, $m_s = 3$ and $u = 2$; (c) shadowing (m_s) with $\bar{\gamma} = \{5, 15\}$ dB, $m = 3$ and $u = 2$. It is worth noting that realistic values of P_f in the range 0 to 0.3 (i.e., low false alarm probability) were mainly considered in Fig. 10. Similarly, Fig. 11 compares the behavior of the differential entropy and AUC for different values of the multipath fading (m) and shadowing (m_s) parameters at $\bar{\gamma} = 2$ and 5 dB. It can be easily seen that the value of the differential entropy increases when the average SNR increases
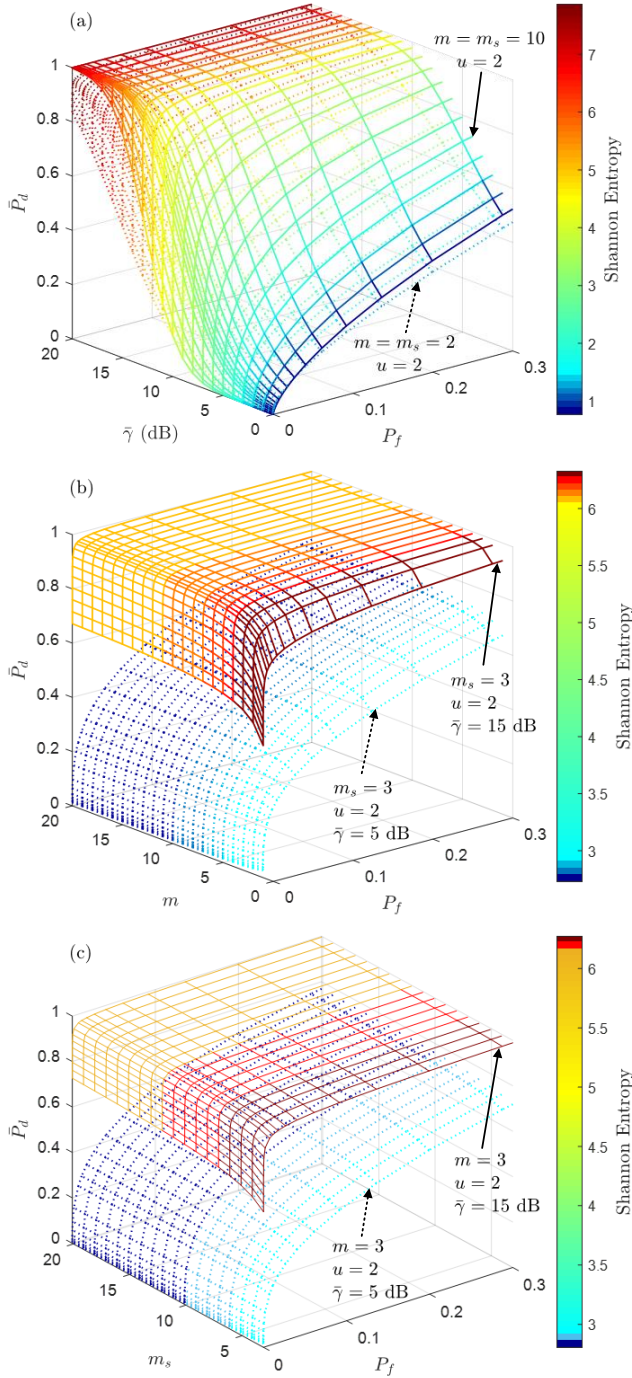
Fig. 10. Behavior of the differential entropy and ROC curves as a function of (a) average SNR ($\bar{\gamma}$), (b) multipath fading (m) and (c) shadowing (m_s) parameters, respectively.

Fig. 11. Behavior of the differential entropy and AUC as a function of multipath fading (m) and shadowing (m_s) parameters at $\bar{\gamma} = \{2, 5\}$ dB.

entropy for different values of the fading parameters at $\bar{\gamma} = 5$, 15 and 25 dB. It is worth remarking that the corresponding average detection probability (when $P_f = 0.1$ and $u = 2$) and AUC are also presented in Table I for the further investigation of the impact of multipath fading, shadowing and average SNR on the energy detection and information content of unknown signals. To obtain the Nakagami-m and Rayleigh fading parameters of the distributions used to encode the $\mathcal{F}$ distribution, we first generated a set of $\mathcal{F}$ RVs and used the maximum likelihood estimation (MLE). The corresponding parameter estimates are also presented in Table I. Interestingly, irrespective of the multipath fading (m) and shadowing (m_s) conditions, the estimated $\bar{\gamma}_R$ and $\bar{\gamma}_N$ are the same as $\bar{\gamma}$. Consequently, the cross entropy between the $\mathcal{F}$ and Rayleigh distributions, i.e., (44), is dependent upon the average SNR only. When comparing the cross entropy for Rayleigh and Nakagami-m, for all of the cases, the Nakagami-m distribution provided lower entropy than the Rayleigh distribution.

From Table I, it is also evident that the differential entropy was smaller than the cross entropy for all of the considered cases. Overall this demonstrates the importance of considering composite fading models when characterization wireless transmission in conventional and emerging communication systems. It is worth remarking that for the light shadowing conditions (e.g., $m_s = 30$), the cross entropy for Nakagami-m distribution is almost the same as the differential entropy. This is due to the fact that the $\mathcal{F}$ distribution coincides with the Nakagami-m distribution when $m_s \to \infty$. Consequently, its relative entropy[7] (also known as the Kullback-Leibler divergence), which is a measure of the distance between two distributions, was close to zero.

VII. Conclusion

In this paper, a comprehensive performance analysis of ED-based spectrum sensing over $\mathcal{F}$ composite fading channels has been carried out. A novel analytic expression for the average energy detection probability was derived and then extended to account for collaborative spectrum sensing, SLS diversity

(higher $\bar{\gamma}$), or when the severity of multipath fading increases (lower m), or when the shadowing conditions become heavier (lower m_s). On the other hand, the values of the average detection probability and AUC increase when the average SNR increase (higher $\bar{\gamma}$), or when the severity of multipath fading decreases (higher m), or when the shadowing conditions become lighter (higher m_s). Consequently, it can be inferred that higher detection capability requires less number of bits for encoding the signal at the same value of $\bar{\gamma}$.

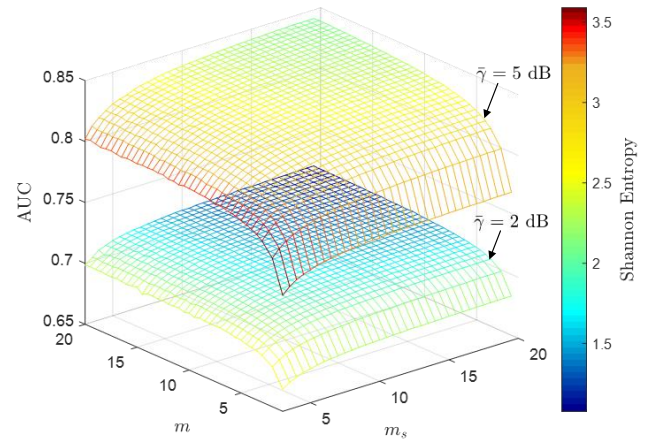Table I depicts the estimated differential entropy and cross

---

[7]The relative entropy is given by $D(p||q) \triangleq H(p, q) - H(p)$ [48].

TABLE I
DIFFERENTIAL ENTROPY AND CROSS ENTROPY FOR DIFFERENT FADING PARAMETERS (m, m_s) AND AVERAGE SNR $(\bar{\gamma})$ ALONG WITH THE AVERAGE DETECTION PROBABILITY$(\bar{P}_d)$, AUC AND THE CORRESPONDING PARAMETER ESTIMATES OF THE RAYLEIGH AND NAKAGAMI-m DISTRIBUTIONS

| $(m, m_s, \bar{\gamma})$ | $H(p)$ | $\bar{P}_d$ | AUC | Rayleigh | | Nakagami-m | | |
				$\bar{\gamma}_R$	$H(p,q)$	m	$\bar{\gamma}_N$	$H(p,q)$
(2, 3, 5 dB)	3.005	0.494	0.772	5 dB	3.104	1.14	5 dB	3.096
(2, 30, 5 dB)	2.959	0.551	0.805	5 dB	3.104	1.89	5 dB	2.960
(20, 3, 5 dB)	2.730	0.537	0.803	5 dB	3.104	2.11	5 dB	2.913
(20, 30, 5 dB)	1.870	0.606	0.845	5 dB	3.104	11.99	5 dB	1.876
(2, 3, 15 dB)	6.327	0.905	0.934	15 dB	6.426	1.14	15 dB	6.418
(2, 30, 15 dB)	6.281	0.978	0.980	15 dB	6.426	1.88	15 dB	6.282
(20, 3, 15 dB)	6.051	0.966	0.969	15 dB	6.426	2.11	15 dB	6.235
(20, 30, 15 dB)	5.191	0.999	0.999	15 dB	6.426	11.98	15 dB	5.198
(2, 3, 25 dB)	9.649	0.954	0.954	25 dB	9.748	1.14	25 dB	9.740
(2, 30, 25 dB)	9.603	0.983	0.983	25 dB	9.748	1.88	25 dB	9.604
(20, 3, 25 dB)	9.374	0.971	0.971	25 dB	9.748	2.12	25 dB	9.557
(20, 30, 25 dB)	8.514	0.999	1.000	25 dB	9.748	11.96	25 dB	8.520

reception and noise power uncertainty. Additionally, as a figure of merit to determine the performance of ED-based spectrum sensing, a closed-form expression for the AUC was also derived. It was shown that the detection performance increased when the average SNR increased, the time-bandwidth product decreased, or when the multipath fading and shadowing severity decreased. As anticipated, the detection performance was significantly improved as the number of diversity branches increased. Furthermore, when more collaborative users shared their local decision information, a better detection performance was achieved for both the OR- and AND-rules. Among these rules, the OR-rule was observed to provide a better detection performance compared to the AND-rule. To validate the analytical expressions presented in the paper, simulation results were also presented.

Most importantly though, it is noted that the analytical form of the average detection probability for ED-based spectrum sensing over the generalized K fading channels given in [20, eq. (7)] is only valid for integer value of m. However, the analytical expression presented in the paper is valid for any m value meaning that ED-based spectrum sensing may now be tested over a much greater range of multipath fading conditions, which is essential in demanding scenarios such as ED-based spectrum sensing and RADAR systems. Additionally, the analytical expression presented in this paper shows much less complexity due to the computation of a smaller number of special functions and a rapidly converging infinite series.

Novel expressions for the differential entropy and cross entropy were also derived in closed-form. The behavior of the differential entropy was evaluated for different values of the key parameters of $\mathcal{F}$ composite fading channels. Similar to the average detection probability and AUC, the differential entropy is expressed in terms of the multipath, shadowing and average SNR parameters. Hence, there is a relationship between the energy and the information content of a signal and how these are affected by the incurred fading conditions. As a result, we compared the differential entropy with the behavior of

ROC and AUC, offering useful insights on the relationship of these measures, i.e., how different fading conditions affect the sensing of the energy of the signal and its information content. More specifically, this can account for the information content difference for small or large variations of the ROC and AUC measures. For example, in critical values of these measures, such around 0.95, small variations can show the direct change of the differential entropy. Conversely, it can indicate how even slight variations of the differential entropy affect the ROC and AUC. Given that these measures are functions of the involved fading parameters and average SNR, these insights are useful in enabling an accurate and robust detector decision. Overall, it was shown that the more bits were required to encode the corresponding message when the channel was subject to higher average SNR, severer multipath fading and heavier shadowing. Moreover, the cross entropy with the Rayleigh and Nakagami-m distributions demonstrated the information loss encountered when the composite fading was not taken into account.

REFERENCES

[1] S. Atapattu, C. Tellambura, and H. Jiang, "Performance of an energy detector over channels with both multipath fading and shadowing," *IEEE Trans. Wireless Commun.*, vol. 9, no. 12, pp. 3662–3670, Dec. 2010.
[2] S. Koteshwara and K. K. Parhi, "Incremental-precision based feature computation and multi-level classification for low-energy internet-of-things," *IEEE J. Emerg. Sel. Topic Circuits Syst (Early Access)*, 2018.
[3] Z. Li *et al.*, "Dynamic compressive wide-band spectrum sensing based on channel energy reconstruction in cognitive internet of things," *IEEE Trans. Ind. Informat.*, vol. 14, no. 6, pp. 2598–2607, Jun. 2018.

[4] L. Yi, X. Deng, M. Wang, D. Ding, and Y. Wang, "Localized confident information coverage hole detection in Internet of things for radioactive pollution monitoring," *IEEE Access*, vol. 5, pp. 18 665–18 674, Sep. 2017.

[5] S. Shukla, A. K. Rao, and N. Srivastava, "A survey on energy detection schemes in cognitive radios," in *Proc. ICETEESES*, Mar. 2016, pp. 223–228.

[6] M. Sardana and A. Vohra, "Analysis of different spectrum sensing techniques," in *Proc. Comptelix*, Jul. 2017, pp. 422–425.

[7] P. D. Sutton, K. E. Nolan, and L. E. Doyle, "Cyclostationary signatures in practical cognitive radio applications," *IEEE J. Sel. Areas Commun.*, vol. 26, no. 1, pp. 13–24, Jan. 2008.

[8] H. Urkowitz, "Energy detection of unknown deterministic signals," *Proc. IEEE*, vol. 55, no. 4, pp. 523–531, Apr. 1967.

[9] A. Ghasemi and E. S. Sousa, "Spectrum sensing in cognitive radio networks: Requirements, challenges and design trade-offs," *IEEE Commun. Mag.*, vol. 46, no. 4, Apr. 2008.

[10] Y.-C. Liang, K.-C. Chen, G. Y. Li, and P. Mahonen, "Cognitive radio networking and communications: An overview," *IEEE Trans. Veh. Technol.*, vol. 60, no. 7, pp. 3386–3407, Sep. 2011.

[11] F. F. Digham, M.-S. Alouini, and M. K. Simon, "On the energy detection of unknown signals over fading channels," in *Proc. IEEE ICC*, May 2003, pp. 3575–3579.

[12] F. B. S. de Carvalho, W. T. A. Lopes, and M. S. Alencar, "Performance of cognitive spectrum sensing based on energy detector in fading channels," *Procedia Comput. Sci.*, vol. 65, pp. 140–147, 2015.

[13] D. Horgan and C. C. Murphy, "Fast and accurate approximations for the analysis of energy detection in Nakagami-m channels," *IEEE Commun. Lett.*, vol. 17, no. 1, pp. 83–86, Jan. 2013.

[14] S. Hussain and X. N. Fernando, "Closed-form analysis of relay-based cognitive radio networks over Nakagami-m fading channels," *IEEE Trans. Veh. Technol.*, vol. 63, no. 3, pp. 1193–1203, Sep. 2014.

[15] F. F. Digham, M.-S. Alouini, and M. K. Simon, "On the energy detection of unknown signals over fading channels," *IEEE Trans. Commun.*, vol. 55, no. 1, pp. 21–24, Jan. 2007.

[16] P. C. Sofotasios *et al.*, "A comprehensive framework for spectrum sensing in non-linear and generalized fading conditions," *IEEE Trans. Veh. Technol*, vol. 66, no. 10, pp. 8615–8631, Oct. 2017.

[17] H. Rasheed, F. Haroon, and N. Rajatheva, "Performance analysis of Rice-lognormal channel model for spectrum sensing," in *Proc. ECTI-CON*, May 2010, pp. 420–424.

[18] S. Atapattu, C. Tellambura, and H. Jiang, "Energy detection based cooperative spectrum sensing in cognitive radio networks," *IEEE Trans. Wireless Commun.*, vol. 10, no. 4, pp. 1232–1241, Apr. 2011.

[19] N. Reisi, S. Gazor, and M. Ahmadian, "Distributed cooperative spectrum sensing in mixture of large and small scale fading channels," *IEEE Trans. Wireless Commun.*, vol. 12, no. 11, pp. 5406–5412, Nov. 2013.

[20] S. Atapattu, C. Tellambura, and H. Jiang, "Performance of an energy detector over channels with both multipath fading and shadowing," *IEEE Trans. Wireless Commun.*, vol. 9, no. 12, pp. 3662–3670, Dec. 2010.

[21] K. P. Peppas, G. Efthymoglou, V. Aalo, M. Alwakeel, and S. Alwakeel, "Energy detection of unknown signals in Gamma-shadowed Rician fading environments with diversity reception," *IET Commun.*, vol. 9, no. 2, pp. 196–210, Jan. 2014.

[22] H. Al-Hmood and H. S. Al-Raweshidy, "Unified modeling of composite κ-μ / gamma, η-μ / gamma and α-μ / gamma fading channels using a mixture gamma distribution with applications to energy detection," *IEEE Antennas and Wireless Propag. Lett.*, vol. 16, pp. 104–108, Feb. 2017.

[23] S. K. Yoo *et al.*, "The Fisher-Snedecor $\mathcal{F}$ distribution: A simple and accurate composite fading model," *IEEE Commun. Lett.*, vol. 21, no. 7, pp. 1661–1664, Jul. 2017.

[24] H. Al-Hmood, "Performance of cognitive radio systems over κ-μ shadowed with integer μ and fisher-snedecor $\mathcal{F}$ fading channels," in *Proc. IICETA*, May 2018, pp. 130–135.

[25] Y.-Y. Zhu and Y.-G. Zhu, "The simulation study of entropy-based signal detector over fading channel," in *Proc. WCSP*, Oct. 2012, pp. 1–5.

[26] I. S. Gradshteyn and I. M. Ryzhik, *Table of Integrals, Series, and Products*, 7th ed. London: Academic Press, 2007.

[27] M. Abramowitz and I. A. Stegun, *Handbook of mathematical functions*. Washington, DC. US Dept. of Commerce, National Bureau of Standards, 1972.

[28] P. E. Cantrell and A. K. Ojha, "Comparison of generalized Q-function algorithms," *IEEE Trans. Inf. Theory*, vol. 33, no. 4, pp. 591–596, Jul. 1987.

[29] V. M. Kapinas, S. K. Mihos, and G. K. Karagiannidis, "On the monotonicity of the generalized Marcum and Nuttall Q-functions," *IEEE Trans. Inf. Theory*, vol. 55, no. 8, pp. 3701–3710, Aug. 2009.

[30] Wolfram Research, Inc., 2018, visited on 07/13/2018. [Online]. Available: http://functions.wolfram.com/id.

[31] A. Ghasemi and E. S. Sousa, "Impact of user collaboration on the performance of sensing-based opportunistic spectrum access," in *Proc. IEEE VTC*, Sep. 2006, pp. 1–6.

[32] D. Duan, L. Yang, and J. C. Principe, "Cooperative diversity of spectrum sensing for cognitive radio systems," *IEEE Trans. Signal Process.*, vol. 58, no. 6, pp. 3218–3227, Jun. 2010.

[33] E. A. Neasmith and N. C. Beaulieu, "New results on selection diversity," *IEEE Trans. Commun.*, vol. 46, no. 5, pp. 695–704, May 1998.

[34] R. Tandra and A. Sahai, "SNR walls for signal detection," *IEEE J. Sel. Topics Signal Process.*, vol. 2, no. 1, pp. 4–17, Feb. 2008.

[35] Y. Xiao and F. Hu, *Cognitive radio networks*. CRC press, 2008.

[36] S. Dikmese, Z. Ilyas, P. C. Sofotasios, M. Renfors, and M. Valkama, "Sparse frequency domain spectrum sensing and sharing based on cyclic prefix autocorrelation," *IEEE J. Sel. Areas Commun.*, vol. 35, no. 1, pp. 159–172, Jan. 2017.

[37] S. Dikmese, P. C. Sofotasios, M. Renfors, and M. Valkama, "Subband energy based reduced complexity spectrum sensing under noise uncertainty and frequency-selective spectral characteristics," *IEEE Trans. Signal Process.*, vol. 64, no. 1, pp. 131–145, Jan. 2016.

[38] M. Lopez-Benitez and F. Casadevall, "Signal uncertainty in spectrum sensing for cognitive radio," *IEEE Trans. Commun.*, vol. 61, no. 4, pp. 1231–1241, Apr. 2013.

[39] T. D. Wickens, *Elementary signal detection theory*. Oxford University Press, USA, 2002.

[40] J. A. Hanley and B. J. McNeil, "The meaning and use of the area under a receiver operating characteristic (ROC) curve," *Radiology*, vol. 143, no. 1, pp. 29–36, Apr. 1982.

[41] S. Dikmese, P. C. Sofotasios, T. Ihalainen, M. Renfors, and M. Valkama, "Efficient energy detection methods for spectrum sensing under non-flat spectral characteristics," *IEEE J. Sel. Areas Commun.*, vol. 33, no. 5, pp. 755–770, May 2015.

[42] S. Atapattu, C. Tellambura, and H. Jiang, "Analysis of area under the ROC curve of energy detection," *IEEE Trans. Wireless Commun.*, vol. 9, no. 3, Mar. 2010.

[43] T. Fawcett, "An introduction to ROC analysis," *Pattern Recognit. Lett.*, vol. 27, no. 8, pp. 861–874, Jun. 2006.

[44] S. Alam, O. Olabiyi, O. Odejide, and A. Annamalai, "A performance study of energy detection for dual-hop transmission with fixed gain relays: area under ROC curve (AUC) approach," in *Proc. IEEE PIMRC*, Sep. 2011, pp. 1840–1844.

[45] P. C. Sofotasios *et al.*, "Entropy and channel capacity under optimum power and rate adaptation over generalized fading conditions," *IEEE Signal Process. Lett.*, vol. 22, no. 11, pp. 2162–2166, Nov. 2015.

[46] J. V. Michalowicz, J. M. Nichols, and F. Bucholtz, *Handbook of differential entropy*. Chapman and Hall/CRC, 2013.

[47] A. V. Lazo and P. Rathie, "On the entropy of continuous probability distributions (corresp.)," *IEEE Trans. Inf. Theory*, vol. 24, no. 1, pp. 120–122, Jan. 1978.

[48] S. Kullback, *Information theory and statistics*. Courier Corporation, 1997.

Seong Ki Yoo (S'14–M'17) received the B.Eng. (Hons.) degree in telecommunication systems from the University of Surrey, Guildford, U.K., in 2010, and the M.Sc. degree in communications and signal processing from Imperial College London, London, U.K., in 2012 and the Ph.D. degree from Queen's University Belfast, Belfast, U.K., in 2017. His Doctoral studies were sponsored by U.K. EPSRC. He was a junior researcher with Korea Electrotechnology Research Institute (KERI), Ansan, South Korea, from 2012 to 2013. He is currently a Post-Doctoral Research Fellow with Centre for Wireless Innovation (CWI), ECIT Institute, Queen's University Belfast. His research interests include mmWave channel modelling and measurements, fading characterization for wearable communications channels and performance analysis over fading channels.

Paschalis C. Sofotasios (S'07-M'12-SM'16) was born in Volos, Greece, in 1978. He received the MEng degree from Newcastle University, UK, in 2004, the MSc degree from the University of Surrey, UK, in 2006, and the PhD degree from the University of Leeds, UK, in 2011. His MSc studies were funded by a scholarship from UK-EPSRC and his PhD studies were sponsored by UK-EPSRC and Pace plc. He has held academic positions at the University of Leeds, UK, University of California at Los Angeles, Los Angeles, USA, Aristotle University of Thessaloniki, Greece, Tampere University of Technology, Finland, and Khalifa University, UAE, where he is currently an Assistant Professor. His research interests include broad areas of digital and optical wireless communications including topics on pure mathematics and statistics.

Dr. Sofotasios has been a member and co-chair of the Technical Program Committee of numerous IEEE conferences. He received an Exemplary Reviewer Award from the IEEE COMMUNICATIONS LETTERS in 2012 and from the IEEE TRANSACTIONS ON COMMUNICATIONS in 2015 and 2016. He is a Senior Member IEEE and was a co-recipient of the Best Paper Award at ICUFN '13. He currently serves as an Editor for the IEEE COMMUNICATIONS LETTERS.

Osamah S. Badarneh (S'06–M'09) received the Ph.D. degree in electrical engineering from the University of Quebec-ETS, Canada, in 2009. He was an Assistant Professor with the Department of Telecommunication Engineering, Yarmouk University, Jordan, from 2010 to 2012. In 2012, he joined the Department of Electrical Engineering, University of Tabuk, Saudi Arabia, where he is currently an Associate Professor. He has served as an Adjunct Professor with the Department of Electrical Engineering, University of Quebec-ETS, since 2013. His research interests focus on wireless communications and networking.

Simon L. Cotton (S'04–M'07–SM'14) received the B.Eng. degree in electronics and software from Ulster University, Ulster, U.K., in 2004, and the Ph.D. degree in electrical and electronic engineering from the Queen's University of Belfast, Belfast, U.K., in 2007. He is currently a Reader in Wireless Communications and the Director of the Centre for Wireless Innovation (CWI), Queen's University Belfast. He has authored and co-authored over 140 publications in major IEEE/IET journals and refereed international conferences, two book chapters, and two patents. Among his research interests are cellular device-to-device, vehicular, and body-centric communications. His other research interests include radio channel characterization and modeling and the simulation of wireless channels. He was a recipient of the H. A. Wheeler Prize, in 2010, from the IEEE Antennas and Propagation Society for the best applications journal paper in the IEEE TRANSACTIONS ON ANTENNAS AND PROPAGATION in 2009. In 2011, he was a recipient of the Sir George Macfarlane Award from the U.K. Royal Academy of Engineering in recognition of his technical and scientific attainment since graduating from his first degree in engineering.

George K. Karagiannidis (M'96-SM'03-F'14) was born in Pithagorion, Samos Island, Greece. He received the University Diploma (5 years) and PhD degree, both in electrical and computer engineering from the University of Patras, in 1987 and 1999, respectively. From 2000 to 2004, he was a Senior Researcher at the Institute for Space Applications and Remote Sensing, National Observatory of Athens, Greece. In June 2004, he joined the faculty of Aristotle University of Thessaloniki, Greece where he is currently Professor in the Electrical Computer Engineering Dept. and Director of Digital Telecommunications Systems and Networks Laboratory. He is also Honorary Professor at South West Jiaotong University, Chengdu, China. His research interests are in the broad area of Digital Communications Systems and Signal processing, with emphasis on Wireless Communications, Optical Wireless Communications, Wireless Power Transfer and Applications, Communications for Biomedical Engineering, Stochastic Processes in Biology and Wireless Security. He is the author or co-author of more than 500 technical papers published in scientific journals and presented at international conferences. He is also author of the Greek edition of a book on Telecommunications Systems and co-author of the book Advanced Optical Wireless Communications Systems, Cambridge Publications, 2012.

Dr. Karagiannidis has been involved as General Chair, Technical Program Chair and member of Technical Program Committees in several IEEE and non-IEEE conferences. In the past, he was Editor in IEEE TRANSACTIONS ON COMMUNICATIONS, Senior Editor of IEEE COMMUNICATIONS LETTERS Editor of the EURASIP JOURNAL OF WIRELESS COMMUNICATIONS & NETWORKS and several times Guest Editor in IEEE SELECTED AREAS IN COMMUNICATIONS. From 2012 to 2015 he was the Editor-in Chief of IEEE COMMUNICATIONS LETTERS. Dr. Karagiannidis is one of the highly-cited authors across all areas of Electrical Engineering, recognized from Clarivate Analytics as Web-of-Science Highly-Cited Researcher in the four consecutive years 2015-2018.

Sami Muhaidat (S'01–M'07–SM'11) received the Ph.D. degree in Electrical and Computer Engineering from the University of Waterloo, Waterloo, Ontario, in 2006. From 2007 to 2008, he was an NSERC postdoctoral fellow in the Department of Electrical and Computer Engineering, University of Toronto, Canada. From 2008-2012, he was an Assistant Professor in the School of Engineering Science, Simon Fraser University, BC, Canada. He is currently an Associate Professor at Khalifa University, and a Visiting Reader (Associate Professor) in the Faculty of Engineering, University of Surrey, UK. Sami's research focuses on wireless communications, optical communications, IoT with emphasis on battery-less devices, and machine learning. Sami is currently an Area Editor for IEEE TRANSACTIONS ON COMMUNICATIONS. He served as a Senior Editor for IEEE COMMUNICATIONS LETTERS, an Editor for IEEE TRANSACTIONS ON COMMUNICATIONS, and an Associate Editor for IEEE TRANSACTIONS ON VEHICULAR TECHNOLOGY. He is also a member of Mohammed Bin Rashid Academy of scientists.